MiniGPT-v2: Large Language Model as a Unified Interface for Vision-Language Multi-task Learning

Anonymous authors
Paper under double-blind review

Abstract

Large language models have shown their remarkable capabilities as a general interface for various language-related applications. Motivated by this, we target to build a unified interface for completing many vision-language tasks including image description, visual question answering, and visual grounding, among others. The challenge for achieving this is to use a single model for performing diverse vision-language tasks effectively with simple multi-modal instructions. To address this issue, we introduce MiniGPT-v2, a model can be treated a unified interface for better handling various vision-language tasks. We propose using unique identifiers for different tasks when training the model. These identifiers enable our model to distinguish each task instruction effortlessly and also improve the model learning efficiency for each task. After our three-stage training, the experimental results show that MiniGPT-v2 achieves strong performance on many visual question answering and visual grounding benchmarks compared to other vision-language generalist models. Our trained models and codes will be made available.

1 Introduction

Multi-modal Large Language Models (LLMs) have emerged as an exciting research topic with a rich set of applications in vision-language community, such as visual AI assistant, image captioning, visual question answering (VQA), and referring expression comprehension (REC). A key feature of multimodal large language models is that they can inherit advanced capabilities (e.g., logical reasoning, common sense, and strong language expression) from the LLMs (OpenAI, 2022; Touvron et al., 2023a;b; Chiang et al., 2023). When tuned with proper vision-language instructions, multi-modal LLMs, specifically vision-language models, demonstrate strong capabilities such as producing detailed image descriptions, generating code, localizing the visual objects in the image, and even perform multi-modal reasoning to better answer complicated visual questions (Zhu et al., 2023b; Liu et al., 2023b; Ye et al., 2023; Wang et al., 2023b; Chen et al., 2023b; Dai et al., 2023; Zhu et al., 2023a; Chen et al., 2023a; Zhuge et al., 2023). This evolution of LLMs enables interactions of visual and language inputs across communication with individuals and has been shown quite effective for building visual chatbots.

However, learning to perform multiple vision-language tasks effectively and formulating their corresponding multi-modal instructions present considerable challenges due to the complexities inherent among different tasks. For instance, given a user input *"tell me the location of a person"*, there are many ways to interpret and respond based on the specific task. In the context of the referring expression comprehension task, it can be answered with one bounding box location of the person. For the visual question answering, the model might describe the spatial location using human natural language. For person detection, the model might identify every spatial location of a human being. To alleviate this issue, we propose a task-oriented instruction training scheme to reduce the multi-modal instructional ambiguity, and a vision-language model, MiniGPT-v2. Specifically, we provide an unique task identifier token for each task. For example, we provide a *[vqa]* identifier token for training all the data samples from the visual question answering tasks. In total, we provide six different task identifiers during the model training stages.

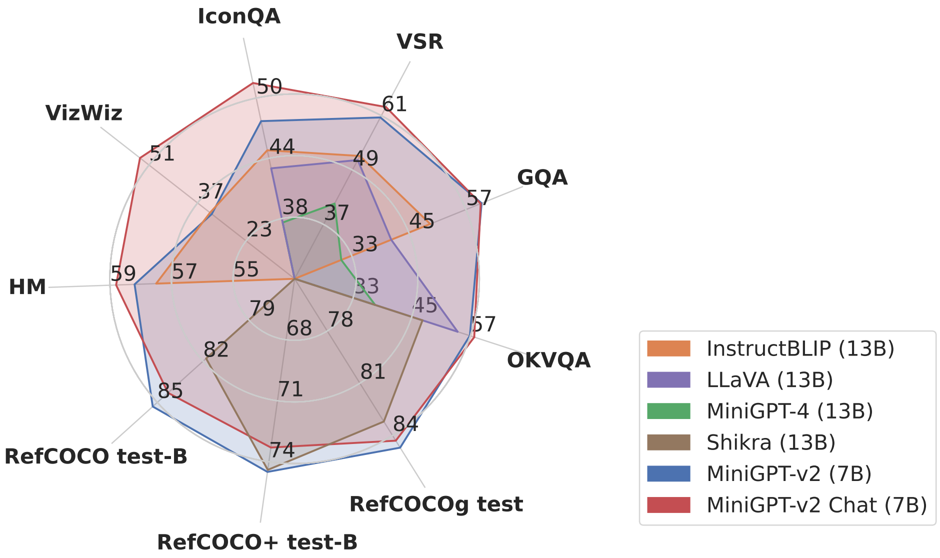

Figure 1: Our MiniGPT-v2 achieves state-of-the-art performances on a broad range of vision-language tasks compared with other generalist models.

Our model, MiniGPT-v2, has a simple architecture design. It directly takes the visual tokens from a ViT vision encoder (Fang et al., 2022) and project them into the feature space of a large language model (Touvron et al., 2023b). For better visual perception, we utilize high-resolution images (448x448) during training. But this will result in a larger number of visual tokens. To make the model training more efficient, we concatenate every four neighboring visual tokens into a single token, reducing the total number by 75%. Additionally, we utilize a three-stage training strategy to effectively train our model with a mixture of weakly-labeled, fine-grained image-text datasets, and multi-modal instructional datasets, with different training focus at each stage.

To evaluate the performance of our model, we conducted extensive experiments on diverse vision-language tasks, including (detailed) image/grounded captioning, vision question answering, and visual grounding. The results demonstrate that our MiniGPT-v2 can achieve SOTA or comparable performance on diverse benchmarks compared to previous vision-language generalist models, such as MiniGPT-4 (Zhu et al., 2023b), InstructBLIP (Dai et al., 2023), LLaVA (Liu et al., 2023b) and Shikra (Chen et al., 2023b). For example, our MiniGPT-v2 outperforms MiniGPT-4 by 21.7%, InstructBLIP by 11.2%, and LLaVA by 12.1% on the VSR benchmark (Liu et al., 2023a), and it also performs better than the previously established strong baseline, Shikra, in most validations on RefCOCO, RefCOCO+, and RefCOCOg. Our model establishes new state-of-the-art results on these benchmarks among vision-language generalist models, shown in Fig. 1.

2 Related Work

We briefly review relevant works on Multi-task generalist models and multi-modal LLMs for visual aligning.

Multi-task generalist models. Recent years have witnessed significant advancements in vision-language learning, particularly in the development of multi-task generalist models (Hu & Singh, 2021; Yu et al., 2022; Lu et al., 2023; Singh et al., 2022; Zhang et al., 2021; Gan et al., 2020; Li et al., 2020; Yuan et al., 2021). These models act as versatile interfaces for a range of vision-language tasks. Unified I/O (Lu et al., 2022) integrates diverse tasks such as segmentation, depth estimation, and vision-language tasks. Florence (Yuan et al., 2021) expands the model training various representations, such as scene, object, images, videos, depths, and vision-language, via the web-scale image-text data training. BEIT-3 (Wang et al., 2022b) brings together various vision-language tasks through masked token prediction. FLAVA (Singh et al., 2022) pioneers a universal model by jointly pretraining on vision tasks, language tasks, and combined vision-language tasks.

ONE-PEACE (Wang et al., 2023a) aligns vision, language, and audio within a cohesive semantic framework. CLIP (Radford et al., 2021), Align Li et al. (2022), OpenCLIP (Ilharco et al., 2021), MetaCLIP (Xu et al., 2023a) align vision and language modalities in a shared semantic space, leveraging contrastive learning on extensive internet data.

Multi-modal large language model (LLM). Large language models (Radford et al., 2019; Devlin et al., 2018; Brown et al., 2020; OpenAI, 2022; Touvron et al., 2023a;b; Chowdhery et al., 2022; OpenAI, 2023) have achieved significant breakthroughs during the past few years. Their exceptional capabilities in generalization and representation have facilitated their expansion into the multi-modal domain by aligning visual inputs with LLMs. Initial efforts such as VisualGPT (Chen et al., 2022) and Frozen (Tsimpoukelli et al., 2021) used pre-trained language models to augment vision-language models for the image captioning and visual question answering. This initial exploration paved the way for subsequent vision-language research such as Flamingo (Alayrac et al., 2022) and BLIP-2 (Li et al., 2023b). More recently, GPT-4(V) (OpenAI, 2023) has been released and demonstrates many advanced multi-modal abilities, e.g., generating website code based on handwritten text instructions, based on its strong language model. Those demonstrated capabilities inspired other vision-language LLMs, including MiniGPT-4 (Zhu et al., 2023b), LLaVA (Liu et al., 2023b), mPLUG-Owl (Ye et al., 2023) and Otter Li et al. (2023a), which align the image inputs also with an advanced large language model with proper multi-modal instructional tuning. These vision-language models also showcase many advanced multi-modal capabilities similar to GPT-4(V). More recent developments include Vision-LLM (Wang et al., 2023b), Kosmos-2 (Peng et al., 2023), Shikra (Chen et al., 2023b), and our concurrent work, Qwen-VL (Bai et al., 2023). These models further explore visual grounding in the context of LLMs, pushing the boundaries of general multi-task vision-language modeling.

3 Method

In this section, we start by introducing our vision-language model, MiniGPT-v2, then discuss the basic idea of a multi-task instruction template with task identifier for training, and finally adapt our task identifier idea to achieve task-oriented instruction tuning.

3.1 Model Architecture

Our proposed model architecture, MiniGPT-v2, is shown in Fig. 2. It consists of three components: a visual backbone, a linear projection layer, and a large language model. We describe each component as follows:

Visual backbone. MiniGPT-v2 adapts the EVA (Fang et al., 2022) as our visual backbone model backbone. We freeze the visual backbone during the entire model training. We train our model with the image resolution 448x448, and we interpolate the positional encoding to scale with higher image resolution.

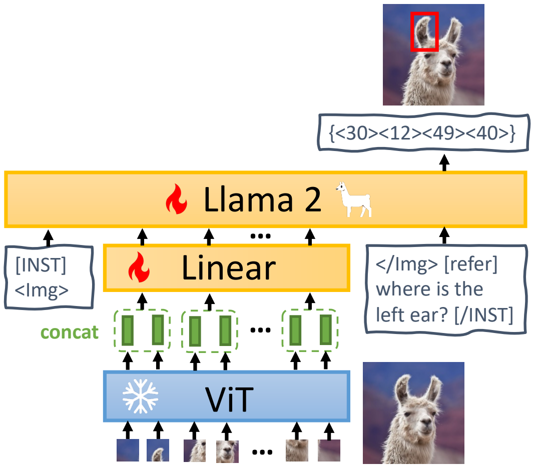

Figure 2: **Architecture of MiniGPT-v2.** The model takes a ViT visual backbone, which remains frozen during all training phases. We concatenate four adjacent visual output tokens from ViT backbone and project them into LLaMA-2 language model space via a linear projection layer.

Linear projection layer. We aim to project all the visual tokens from the frozen vision backbone into the language model space. However, for higher-resolution images such as 448x448, projecting all the image tokens will result in a very long-sequence input (e.g., 1024 tokens) and significantly lowers the training and inference efficiency. To improve the efficiency, we simply concatenate 4 adjacent visual tokens in the embedding space and project them together into one single embedding in the same feature space of the large language model, thus reducing the number of visual input tokens by 4 times. With this operation, our MiniGPT-v2 can process high-resolution images much more efficiently during the training and inference stage.

Large language model. MiniGPT-v2 adopts the open-sourced LLaMA2-chat (7B) (Touvron et al., 2023b) as the language model backbone. In our work, the language model is treated as a unified interface for various vision-language inputs. We directly rely on the LLaMA-2 language tokens to perform various vision-language tasks. For the visual grounding tasks that necessitate the generation of spatial locations, we directly ask the language model to produce textual representations of bounding boxes to denote their spatial positions.

3.2 Multi-task Instruction Template

When training a single unified model for multiple different tasks such as visual question answering, image caption, referring expression, grounded image caption, and region identification, the multi-modal model might fail to distinguish each task by just aligning visual tokens to language models. For instance, when you ask "Tell me the spatial location of the person wearing a red jacket?", the model can either respond you the location in a bounding box format (e.g., $<\mathrm{X}_{left}><\mathrm{Y}_{top}><\mathrm{X}_{right}><\mathrm{Y}_{bottom}>$) or describe the object location using natural language (e.g., upper right corner). To reduce such ambiguity and make each task easily distinguishable, we introduce task-specific tokens in our designed multi-task instruction template for training. We now describe our multi-task instruction template in more details.

General input format. We follow the LLaMA-2 conversation template design and adapt it for the multi-modal instructional template. The template is denoted as follows,

[INST] <Img> < ImageFeature> </Img> [Task Identifier] Instruction [/INST]

In this template, *[INST]* is considered as the user role, and *[/INST]* is considered as the assistant role. We structure the user input into three parts. The first part is the image features, the second part is the task identifier token, and the third part is the instruction input.

Task identifier tokens. Our model takes a distinct identifier for each task to reduce the ambiguity across various tasks. As illustrated in Table 1, we have proposed six different task identifiers for visual question answering, image caption, grounded image captioning, referring expression comprehension, referring expression generation, and phrase parsing and grounding respectively. For vision-irrelevant instructions, our model does not use any task identifier token.

Tasks	VQA	Caption	Grounded Caption	REC	REG	Object Parsing and Grounding
Identifiers	[vqa]	[caption]	[grounding]	[refer]	[identify]	[detection]

Table 1: Task identifier tokens for 6 different tasks, including visual question answering, image captioning, , grounded image captioning, referring expression comprehension (REC), referring expression generation (REG), and object parsing and grounding (where the model extracts objects from the input text and determines their bounding box locations).

Spatial location representation. For tasks such as referring expression comprehension (REC), referring expression generation (REG), and grounded image captioning, our model is required to identify their spatial location of objects accurately. We represent the spatial location through the textual formatting of bounding boxes in our setting and do not use any new vocabulary tokens, specifically: "$\{<\mathrm{X}_{left}><\mathrm{Y}_{top}><\mathrm{X}_{right}><\mathrm{Y}_{bottom}>\}$". Coordinates for X and Y are represented by integer values normalized in the range [0,100]. $<\mathrm{X}_{left}>$ and $<\mathrm{Y}_{top}>$ denote the x and y coordinate top-left corner of the generated bounding box, and $<\mathrm{X}_{right}>$ and $<\mathrm{Y}_{bottom}>$ denote the x and y coordinates of the bottom-right corner.

3.3 Multi-task Instruction Training

We now adapt our designed multi-task instruction template for instruction training. The basic idea is to take instruction with task-specific identifier token as input for task-oriented instruction training of MiniGPT-v2. When input instructions have task identifier tokens, our model will become more prone to multiple-task understanding during training. We train our model with task identifier instructions for better visual aligment in three stages. The first stage is to help MiniGPT-v2 build broad vision-language knowledge through many weakly-labeled image-text datasets, and high-quality fine-grained vision-language annotation datasets as well (where we will assign a high data sampling ratio for weakly-labeled image-text datasets). The second stage is to improve the model with only fine-grained data for multiple tasks. The third stage is to finetune our model with more multi-modal instruction and language datasets for answering diverse multi-modal instructions better and behaving as a multi-modal chatbot. The datasets used for training at each stage are listed in the Table 2.

Data types	Dataset	Stage 1	Stage 2	Stage 3
Weakly-labeled	GRIT-20M (REC and REG), LAION, CC3M, SBU	✓	✗	✗
Grounded caption	GRIT-20M	✓	✗	✗
Caption	COCO caption, TextCaps	✓	✓	✓
REC	RefCOCO, RefCOCO+, RefCOCOg, Visual Genome	✓	✓	✓
REG	RefCOCO, RefCOCO+, RefCOCOg	✓	✓	✓
VQA	GQA, VQAv2, OCR-VQA, OK-VQA, AOK-VQA	✓	✓	✓
Multimodal instruction	LLaVA dataset, Flickr30k, Multi-task conversation	✗	✗	✓
Langauge dataset	Unnatural Instructions	✗	✗	✓

Table 2: The training datasets used for our model three-stage training.

Stage 1: Pretraining. To have broad vision-language knowledge, our model is trained on a mix of weakly-labeled and fine-grained datasets. We give a high sampling ratio for weakly-labeled datasets to gain more diverse knowledge in the first-stage.

For the weakly-labeled datasets, we use LAION (Schuhmann et al., 2021), CC3M (Sharma et al., 2018), SBU (Ordonez et al., 2011), and GRIT-20M from Kosmos v2 (Peng et al., 2023) that built the dataset for referring expression comprehension (REC), referring expression generation (REG), and grounded image captioning. The format for grounded image caption is represented like this: *a <p>wooden table</p>*$\{<X_{left}><Y_{top}><X_{right}><Y_{bottom}>\}$ *in the center of the room.*

For fine-grained datasets, we use datasets like COCO caption (Lin et al., 2014) and TextCaps (Sidorov et al., 2020) for image captioning, RefCOCO (Kazemzadeh et al., 2014), RefCOCO+ (Yu et al., 2016), and RefCOCOg (Mao et al., 2016) for REC. For REG, we restructured the data from ReferCOCO and its variants, reversing the order from phrase → bounding boxes to bounding boxes → phrase. For VQA datasets, our training takes a variety of datasets, such as GQA (Hudson & Manning, 2019), VQA-v2 (Goyal et al., 2017), OCR-VQA (Mishra et al., 2019), OK-VQA (Marino et al., 2019), and AOK-VQA (Schwenk et al., 2022).

Stage 2: Multi-task training. To improve the performance of MiniGPT-v2 on each task, we only focus on using fine-grained datasets to train our model at this stage. We exclude the weakly-supervised datasets such as GRIT-20M and LAION from stage-1 and update the data sampling ratio according to frequency of each task. This strategy enables our model to prioritize high-quality aligned image-text data for superior performance across various tasks.

Stage 3: Multi-modal instruction tuning. Subsequently, we focus on tuning our model with more multi-modal instruction dataset and enhance its conversation ability as a chatbot. We continue using the datasets from the second stage, and add instructional datasets, including LLaVA (Liu et al., 2023b), Flickr30k dataset (Plummer et al., 2015), our constructed mixing multi-task dataset, and the language dataset, Unnatural Instruction (Honovich et al., 2022). We give a lower data sampling ratio for the fine-grained datasets from stage-2 and a higher data sampling ratio for the new instruction datasets.

– LLaVA instruction data. We add the multi-modal instruction tuning datasets, including the detailed descriptions and complex reasoning from LLaVA (Liu et al., 2023b), with 23k and 58k data examples respectively.

– Flicker 30k. After the second-stage training, our MiniGPT-v2 can effectively generate the grounded image caption. Nevertheless, these descriptions tend to be short and often cover very few number of visual objects. This is because the GRIT-20M dataset from KOSMOS-v2 (Peng et al., 2023) that our model was trained with, features a limited number of grounded visual objects in each caption, and our model lacks proper multi-modal instruction tuning to teach it to recognize more visual objects. To improve this, we fine-tune our model using the Flickr30k dataset (Plummer et al., 2015), which provides more contextual grounding of entities within its captions.

We prepare the Flickr30k dataset in two distinct formats for training our model to perform grounded image caption and a new task "object parsing and grounding":

1) **Grounded image caption.** We select captions with a minimum of five grounded phrases, containing around 3k samples, and we directly instruct the model to produce the grounded image caption. *a <p>wooden table</p>*$\{<X_{left}><Y_{top}><X_{right}><Y_{bottom}>\}$ *in the center of the room.* The format for grounded image caption is

2) **Object parsing and grounding.** This new task is to parse all the objects from an input caption and then ground each object. To enable this, we simply use the task identifier*[detection]* to differentiate this capability from other tasks. Also, we use Flickr30k to construct two types of instruction datasets: caption$\rightarrow$ grounded phrases and phrase $\rightarrow$ grounded phrase, each containing around 3k and 4k samples. Then we prompt our model with the instruction: *"[detection] description"*, the model will directly parse the objects from the input image description and also ground the objects into bounding boxes.

– Mixing multi-task dataset. After extensive training with single-round instruction-answer pairs, the model might not handle multiple tasks well during multi-round conversations since the context becomes more complex. To alleviate this situation, we create a new multi-round conversation dataset by mixing the data from different tasks. We include this dataset into our third-stage model training.

– Unnatural instruction. The conversation abilities of language model can be reduced after extensive vision-language training. To fix this, we add the language dataset, Unnatural Instruction (Honovich et al., 2022) into our model's third-stage training for helping recover the language generation ability.

4 Experiments

In this section, we present experimental settings and results. We primarily conduct experiments on (detailed) image/grounded captioning, vision question answering, and visual grounding tasks, including referring expression comprehension. We present both quantitative and qualitative results.

Implementation details. Throughout the entire training process, the visual backbone of MiniGPT-v2 remains frozen. We focus on training the linear projection layer and efficient finetuning the language model using LoRA (Hu et al., 2021). With LoRA, we finetune $\mathcal{W}_q$ and $\mathcal{W}_v$ via low-rank adaptation. In our implementation, we set the rank, $r = 64$. We trained the model with an image resolution of 448x448 during all stages. During each stage, we use our designed multi-modal instructional templates for various vision-language tasks during the model training.

Training and hyperparameters. We use AdamW optimizer with a cosine learning rate scheduler to train our model. In the initial stage, we train on 8xA100 GPUs for 400,000 steps with a global batch size of 96 and an maximum learning rate of 1e-4. This stage takes around 90 hours. During the second stage, the model is trained for 50,000 steps on 4xA100 GPUs with a maximum learning rate of 1e-5, adopting a global batch size of 64, and this training stage lasts roughly 20 hours. For the last stage, training is executed for another 50,000 steps on 4xA100 GPUs, using a global batch size of 24 and this training stage took around 10 hours, maintaining the same maximum learning rate of 1e-5.

4.1 Quantitative Evaluation

Dataset and evaluation metrics. We evaluate our model across a range of VQA and visual grounding benchmarks. For VQA benchmarks, we consider OKVQA (Schwenk et al., 2022), GQA (Hudson & Manning, 2019), VSR (Liu et al., 2023a), IconVQA (Lu et al., 2021), VizWiz (Gurari et al., 2018), HatefulMemes (Kiela et al., 2020), and TextVQA (Singh et al., 2019). For visual grounding, we evaluate our model on RefCOCO (Kazemzadeh et al., 2014) and RefCOCO+(Yu et al., 2016), and RefCOCOg(Mao et al., 2016) benchmarks. More details about the dataset and evaluation metrics can be found in the appendix.

Visual question answering results. Table 3 presents our experimental results on multiple VQA benchmarks. Our results compare favorably to baselines including MiniGPT-4 (Zhu et al., 2023b), Shikra (Chen et al., 2023b), LLaVA (Liu et al., 2023b), mPLUG-Owl (Ye et al., 2023), Otter (Li

Method	Grounding	OKVQA	GQA	VSR (zero-shot)	TextVQA (zero-shot)	IconVQA (zero-shot)	VizWiz (zero-shot)	HM (zero-shot)
Flamingo-9B	✗	44.7	-	31.8	-	-	28.8	57.0
BLIP-2 (13B)	✗	45.9	41.0	50.9	42.5	40.6	19.6	53.7
mPLUG-Owl (7B)	✗	22.9	14.0	11.6	38.8	11.6	39.0	-
Otter (7B)	✗	49.0	38.1	6.4	21.5	38.2	50.0	-
InstructBLIP (13B)	✗	-	49.5	52.1	50.7	44.8	33.4	57.5
MiniGPT-4 (13B)	✗	37.5	30.8	41.6	19.4	37.6	-	-
LLaVA (13B)	✗	54.4	41.3	51.2	38.9	43.0	-	-
Shikra (13B)	✓	47.2	-	-	-	-	-	-
Ours (7B)	✓	**56.9**	**60.3**	60.6	51.9	47.7	30.3	58.2
Ours (7B)-chat	✓	55.9	58.8	**63.3**	**52.3**	**49.4**	**53.0**	**59.5**

Table 3: **Results on multiple VQA tasks.** We report top-1 accuracy for each task. Grounding column indicates whether the model incorporates visual localization capability. The best performance for each benchmark is indicated in **bold**.

Method	Model types	RefCOCO			RefCOCO+			RefCOCOg		Avg
		val	test-A	test-B	val	test-A	test-B	val	test	
UNINEXT	Specialist models	92.64	94.33	91.46	85.24	89.63	79.79	88.73	89.37	88.90
G-DINO-L		90.56	93.19	88.24	82.75	88.95	75.92	86.13	87.02	86.60
VisionLLM-H	Generalist models	-	86.70	-	-	-	-	-	-	-
OFA-L		79.96	83.67	76.39	68.29	76.00	61.75	67.57	67.58	72.65
Shikra (7B)		87.01	90.61	80.24	81.60	87.36	72.12	82.27	82.19	82.93
Shikra (13B)		87.83	91.11	81.81	**82.89**	**87.79**	74.41	82.64	83.16	83.96
Ours (7B)		**88.69**	**91.65**	**85.33**	79.97	85.12	**74.45**	**84.44**	**84.66**	**84.29**
Ours (7B)-chat		87.18	90.51	84.57	78.69	84.25	73.23	81.88	83.25	82.95

Table 4: **Results on referring expression comprehension tasks.** Our MiniGPT-v2 outperforms many VL-generalist models including VisionLLM (Wang et al., 2023b), OFA (Wang et al., 2022a) and Shikra (Chen et al., 2023b) and reduces the accuracy gap comparing to specialist models including UNINEXT (Yan et al., 2023) and G-DINO (Liu et al., 2023c).

et al., 2023a) and InstructBLIP (Dai et al., 2023) across all the VQA tasks. The results for mPLUG-Owl, Otter and MiniGPT-4 are borrowed from (Xu et al., 2023b) For example, on QKVQA, our MiniGPT-v2 outperforms MiniGPT-4, Shikra, LLaVA, mPLUG-Owl, Otter and BLIP-2 by 19.4%, 9.7%, 2.5%, 34%, 7.9% and 11%. These results indicate the strong visual question answering capabilities of our model. Furthermore, we find that our MiniGPT-v2 (chat) variant shows higher performance than the version trained after the second stage. On VSR, TextVQA, IconVQA, VizWiz, and HM, MiniGPT-v2 (chat) outperforms MiniGPT-v2 by 2.7%, 0.4%, 1.7%, 12.1%, and 1.3%. We believe that the better performance can be attributed to the improved language skills during the third-stage training, which is able to benefit visual question comprehension and response, especially on VizWiz with 12.1% top-1 accuracy increase.

Referring expression comprehension results. Table 4 compares our model to baselines on REC benchmarks. Our MiniGPT-v2 shows strong REC performance on RefCOCO, RefCOCO+, and RefCOCOg, performing better than other vision-language generalist models. MiniGPT-v2 outperforms OFA-L (Wang et al., 2022a) by over 8% accuracy across all tasks of RefCOCO/RefCOCO+/RefCOCOg. Compared with a strong baseline, Shikra (13B) (Chen et al., 2023b), our model still shows better results, e.g., 84.29% vs 83.96% accuracy in average. These results provide direct evidence for the competing visual grounding capabilities of MiniGPT-v2. Although our model underperforms specialist models, the promising performance indicates its growing competence in visual grounding.

Ablation on task identifier. We conduct ablation studies on the effect of the task identifier on the performance of MiniGPT-v2. We compare our model with the variant without using task identifiers on VQA benchmarks. Both models were trained on 4xA100 GPUs for 24 hours with an equal number of training steps for multiple vision-language tasks. Results in Table 5 demonstrate the performance on multiple VQA benchmarks and consistently show that token identifier training benefits the overall performance of MiniGPT-v2. Specifically, our MiniGPT-v2 with task-oriented instruction training achieves 1.2% top-1 accuracy improvement on average. These ablation results

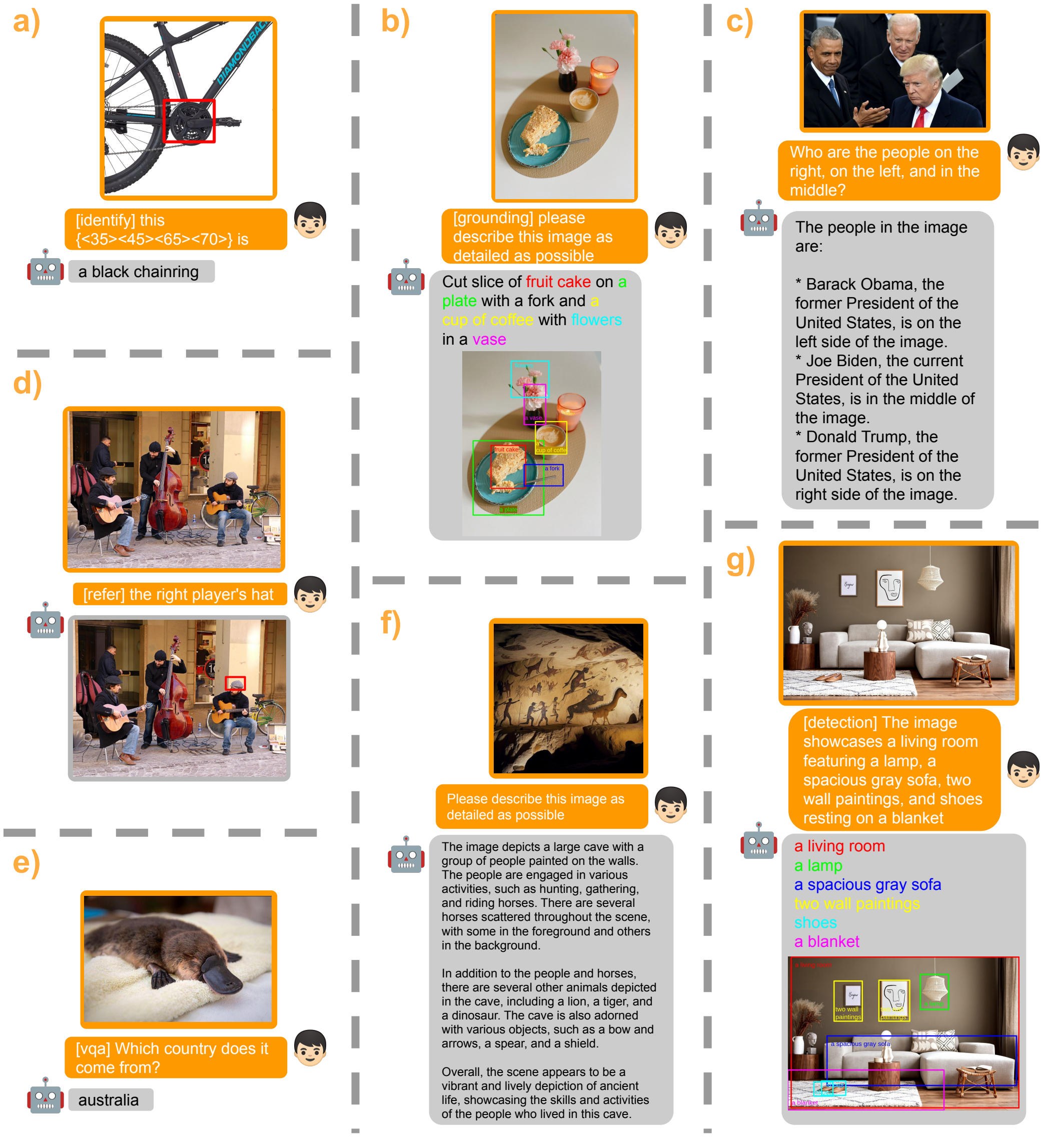

a)

[identify] this {<35><45><65><70>} is

a black chainring

d)

[refer] the right player's hat

e)

[vqa] Which country does it come from?

australia

b)

[grounding] please describe this image as detailed as possible

Cut slice of fruit cake on a plate with a fork and a cup of coffee with flowers in a vase

f)

Please describe this image as detailed as possible

The image depicts a large cave with a group of people painted on the walls. The people are engaged in various activities, such as hunting, gathering, and riding horses. There are several horses scattered throughout the scene, with some in the foreground and others in the background.

In addition to the people and horses, there are several other animals depicted in the cave, including a lion, a tiger, and a dinosaur. The cave is also adorned with various objects, such as a bow and arrows, a spear, and a shield.

Overall, the scene appears to be a vibrant and lively depiction of ancient life, showcasing the skills and activities of the people who lived in this cave.

c)

Who are the people on the right, on the left, and in the middle?

The people in the image are:

* Barack Obama, the former President of the United States, is on the left side of the image.
* Joe Biden, the current President of the United States, is in the middle of the image.
* Donald Trump, the former President of the United States, is on the right side of the image.

g)

[detection] The image showcases a living room featuring a lamp, a spacious gray sofa, two wall paintings, and shoes resting on a blanket

a living room
a lamp
a spacious gray sofa
two wall paintings
shoes
a blanket

Figure 3: **Examples for various multi-modal capabilities of MiniGPT-v2.** We showcase that our model is capable of completing multiple tasks such as referring expression comprehension, referring expression generation, detailed grounded image caption, visual question answering, detailed image description, and directly parsing phrase and grounding from a given input text.

can validate the clear advantage of adding task identifier tokens and support the use of multi-task identifiers for multi-task learning efficiency.

	OKVQA	GQA	VizWiz	VSR	IconVQA	HM	Average
Ours w/o task identifier	50.5	53.4	28.6	57.5	44.8	56.8	48.6
Ours	**52.1**	**54.6**	**29.4**	**59.9**	**45.6**	**57.4**	**49.8**

Table 5: Task identifier ablation study on VQA benchmarks. With task identifier during the model training can overall improve VQA performances from multiple VQA benchmarks

Method	CHAIR$_I$ ↓	CHAIR$_S$ ↓	Len
MiniGPT-4	9.2	31.5	116.2
mPLUG-Owl	30.2	76.8	98.5
LLaVA	18.8	62.7	90.7
MultiModal-GPT	18.2	36.2	45.7
MiniGPT-v2 (long)	8.7	25.3	56.5
MiniGPT-v2 (grounded)	7.6	12.5	18.9
MiniGPT-v2 (short)	**4.4**	**7.1**	**10.3**

Table 6: **Results on hallucination.** We evaluate the hallucination of MiniGPT-v2 with different instructional templates and output three versions of captions for evaluation. For the "long" version, we use the prompt *generate a brief description of the given image*. For the "grounded" version, the instruction is *[grounding] describe this image in as detailed as possible*. For the "short" version, the prompt is *[caption] briefly describe the image*.

Hallucination. We measure the hallucination of our model on image description generation and compare the results with other vision-language baselines, including MiniGPT-4 (Zhu et al., 2023b), mPLUG-Owl (Ye et al., 2023), LLaVA (Liu et al., 2023b), and MultiModal-GPT (Gong et al., 2023). Following the methodology from (Li et al., 2023c), we use CHAIR (Rohrbach et al., 2018) to assess hallucination at both object and sentence levels. As shown in Table 6, we find that our MiniGPT-v2 tends to generate the image description with reduced hallucination compared to other baselines. We have evaluated three types of prompts in MiniGPT-v2. First, we use the prompt *generate a brief description of the given image* without any specific task identifier which tends to produce more detailed image descriptions. Then we provide the instruction prompt *[grounding] describe this image in as detailed as possible* for evaluating grounded image captions. Lastly, we prompt our model with *[caption] briefly describe the image*. With these task identifiers, MiniGPT-v2 is able to produce a variety of image descriptions with different levels of hallucination. As a result, all these three instruction variants have lower hallucination than our baseline, especially with the task specifiers of *[caption]* and *[grounding]*.

4.2 Qualitative Results

We now provide the qualitative results for a complementary understanding of our model's multi-modal capabilities. Some examples can be seen in Fig. 3. Specifically, we demonstrated various abilities in the examples including a) object identification; b) detailed grounded image captioning; c) visual question answering; d) referring expression comprehension; e) visual question answering under task identifier; f) detailed image description; g) object parsing and grounding from an input text. More qualitative results can be found in the Appendix. These results demonstrate that our model has competing vision-language understanding capabilities. Moreover, notice that we train our model only with a few thousand of instruction samples on object parsing and grounding tasks at the third-stage, and our model can effectively follow the instructions and generalize on the new task. This indicates that our model has the flexibility to adapt on many new tasks.

5 Conclusion and Discussion

In this paper, we introduce MiniGPT-v2, a multi-modal LLM that can serve as a unified interface for various vision-language multi-tasking learning. To develop a single model capable of handling multiple vision-language tasks, we propose using distinct identifiers for each task during the training and inference. These identifiers help our model easily differentiate various tasks and also improve the learning efficiency. Our MiniGPT-v2 achieves strong results across many visual question answering and referring expression comprehension benchmarks. We also found that our model can efficiently adapt to new vision-language task, which suggests that MiniGPT-v2 has many potential applications in vision-language community.

However, our model still occasionally shows hallucinations when generating the image description, visual grounding or answering visual questions. e.g., our model may sometimes produce descriptions of non-existent visual objects or generate inaccurate visual locations of grounded objects. We believe aligning the models with more high-quality image-text aligned data, and integrating with a stronger vision backbone and large language model hold the potential for alleviating this issue.

In the appendix, we provide more qualitative results that are generated from our model to demonstrate the vision-language multi-tasking capabilities.

A EVALUATION METRICS

Visual Question Answering (VQA): For the VQA benchmarks, we adopted the standard open-ended VQA evaluation metrics. This involves comparing the model's response directly with the ground truth, and we report the top-1 accuracy as a measure of performance.

RefCOCO/+/g: In assessing visual grounding, we implemented a two-step process. Initially, our model generates a bounding box for each answer, which is then evaluated through the Intersection over Union (IoU) method. We specifically measure the overlap between the generated and ground-truth bounding boxes, considering overlaps greater than 0.5 as indicative of correct grounding.

Hallucination Evaluation: To address the critical aspect of hallucination in generated responses, we employed $CHAIR_i$ and $CHAIR_s$ metrics. $CHAIR_i$ calculates the proportion of hallucinated objects relative to all mentioned objects, offering insight into the frequency of hallucination occurrences. Conversely, $CHAIR_s$ assesses the ratio of captions containing hallucinated objects to the total number of captions, providing a broader view of the model's overall tendency towards hallucination. Here is how $CHAIR_i$ and $CHAIR_s$ are calculated

$$CHAIR_i = \frac{|\{\text{hallucinated objects}\}|}{|\{\text{all mentioned objects}\}|},$$

$$CHAIR_s = \frac{|\{\text{captions with hallucinated objects}\}|}{|\{\text{all captions}\}|},$$

B DATASET DETAILS

Training data. Here we demonstrate the statistics

- GQA (Hudson & Manning, 2019): VQA on scene understanding and reasoning. 22M questions.
- VQAv2 (Goyal et al., 2017): VQA on natural images. 443,757 questions.
- OCR-VQA (Mishra et al., 2019): VQA on images of book covers. 1,002,146 questions.
- OK-VQA (Schwenk et al., 2022): VQA on natural images requiring outside knowledge. 14K questions.
- AOK-VQA (Schwenk et al., 2022): Augmented VQA on natural images requiring outside knowledge. 25K questions.
- LLaVA (Liu et al., 2023b) instruction: 23k detailed descriptions and 58k complex reasoning examples.
- LAION (Schuhmann et al., 2021): CLIP-filtered 400 million image-text pairs.
- CC3M (Sharma et al., 2018): It contains 3.3M web images annotated with captions.
- SBU (Ordonez et al., 2011): A large captioned photo collection with 1 million images on Flickr.
- COCO caption (Lin et al., 2014): It consists of a half million captions describing over 330,000 images.
- TextCaps (Sidorov et al., 2020): It contains 28,408 images from OpenImages, 142,040 captions.
- Flickr30K (Plummer et al., 2015) contains 31,783 images.
- RefCOCO (Kazemzadeh et al., 2014) contains 142,209 referring expression for 50,000 objects in 19,994 images.

- RefCOCOg (Mao et al., 2016) contains 85,474 referring expression for 54,822 objects in 26,711 images
- RefCOCO+ (Yu et al., 2016) contains 141,564 referring expression for 49,856 objects in 19,992 images
- GRIT 20M (Peng et al., 2023) it contains around 20M grounded image caption.

C Instruction template for various vision-language tasks

RefCOCO/RefCOCO+/RefCOCOg: *[refer] give me the location of* {*question*}

VizWiz: *[vqa] Based on the image, respond to this question with a short answer:* {*question*} *and reply 'unanswerable' if you could not answer it*

Hateful Meme: *[vqa] This is an image with:* {*question*} *written on it. Is it hateful? Answer:*

VSR: *[vqa] Based on the image, is this statement true or false?* {*question*}

IconQA, GQA, OKVQA: *[vqa] Based on the image, respond to this question with a short answer:* {*question*}

D MiniGPT-v2 conversation evaluation

We evaluate MiniGPT-v2 under a multi-round conversation, and we demonstrate the conversation in the Fig. 4

E Additional Qualitative Results

To study how well our model is able to take visual input and answer questions based on task-oriented identifier, we use our model to perform multiple vision-language tasks including grounded image captioning in Fig. 5, Fig. 6, Fig. 7 and Fig. 8; Object parsing and grounding in Fig. 9, Fig. 10, Fig. 11 and Fig. 12; Referring expression comprehension in Fig. 13, Fig. 14, Fig. 15 and Fig. 16; Object identification in Fig. 17, Fig. 18, Fig. 19 and Fig. 20.

For each task, we share 4 examples for showing the vision-language capabilities of our model. The results in the demo provide direct evidence for the competing visual understanding capabilities of MiniGPT-v2 on multiple vision-language tasks. For example, in the cases of grounded caption, our model is able to give correct grounded image caption with detailed spatial locations of objects. In the cases of identify, the model also generates our expected object names. MiniGPT-v2 can understand the new scenes and follow the question identifier to respond. But we also need to note that our model still has some hallucination e.g., In Fig. 7, several persons are not grounded accurately, and in Fig. 8, there does not exist a vase in the image.

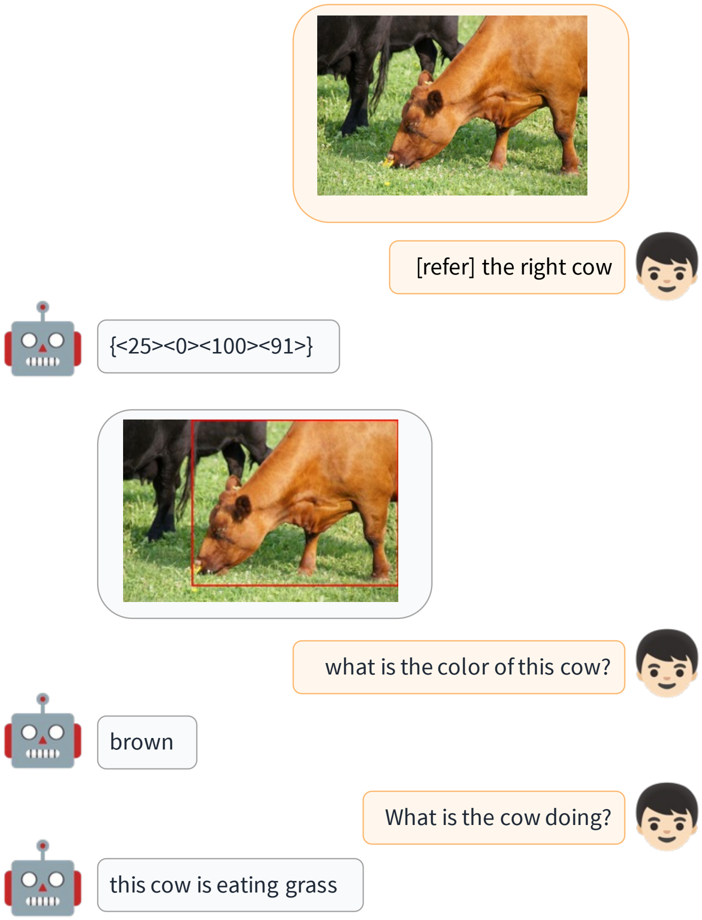

[refer] the right cow

{<25><0><100><91>}

what is the color of this cow?

brown

What is the cow doing?

this cow is eating grass

Figure 4: Conversation evaluation.

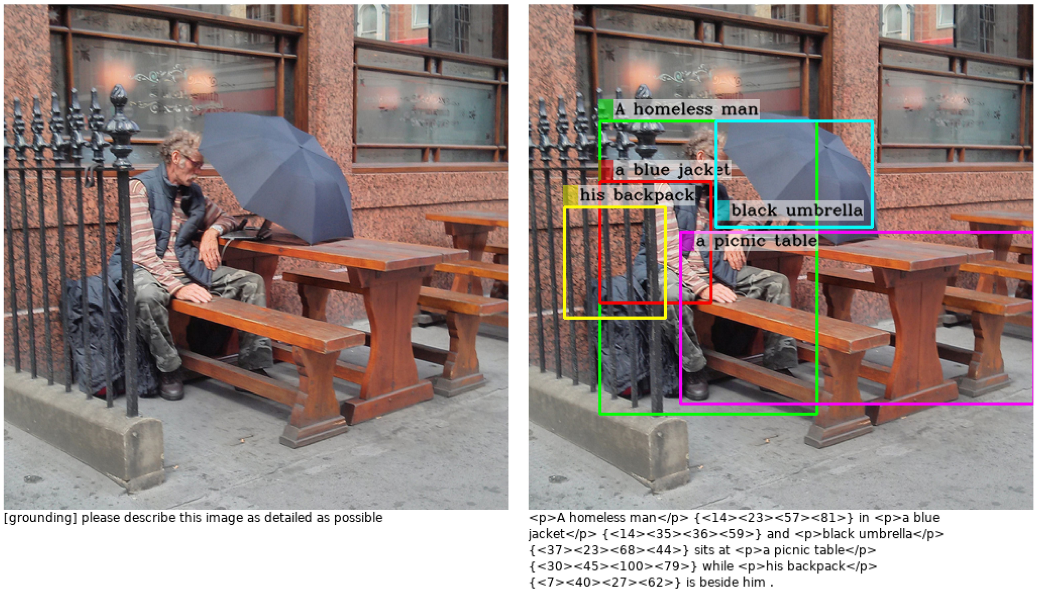

[grounding] please describe this image as detailed as possible

```
<p>A homeless man</p> {<14><23><57><81>} in <p>a blue
jacket</p> {<14><35><36><59>} and <p>black umbrella</p>
{<37><23><68><44>} sits at <p>a picnic table</p>
{<30><45><100><79>} while <p>his backpack</p>
{<7><40><27><62>} is beside him .
```

Figure 5: Detail grounded image caption example.

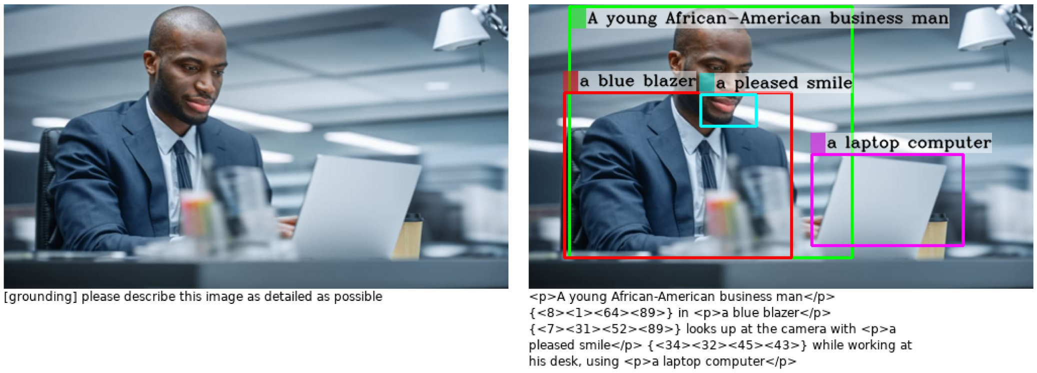

[grounding] please describe this image as detailed as possible

```
<p>A young African-American business man</p>
{<8><1><64><89>} in <p>a blue blazer</p>
{<7><31><52><89>} looks up at the camera with <p>a
pleased smile</p> {<34><32><45><43>} while working at
his desk, using <p>a laptop computer</p>
```

Figure 6: Detail grounded image caption example

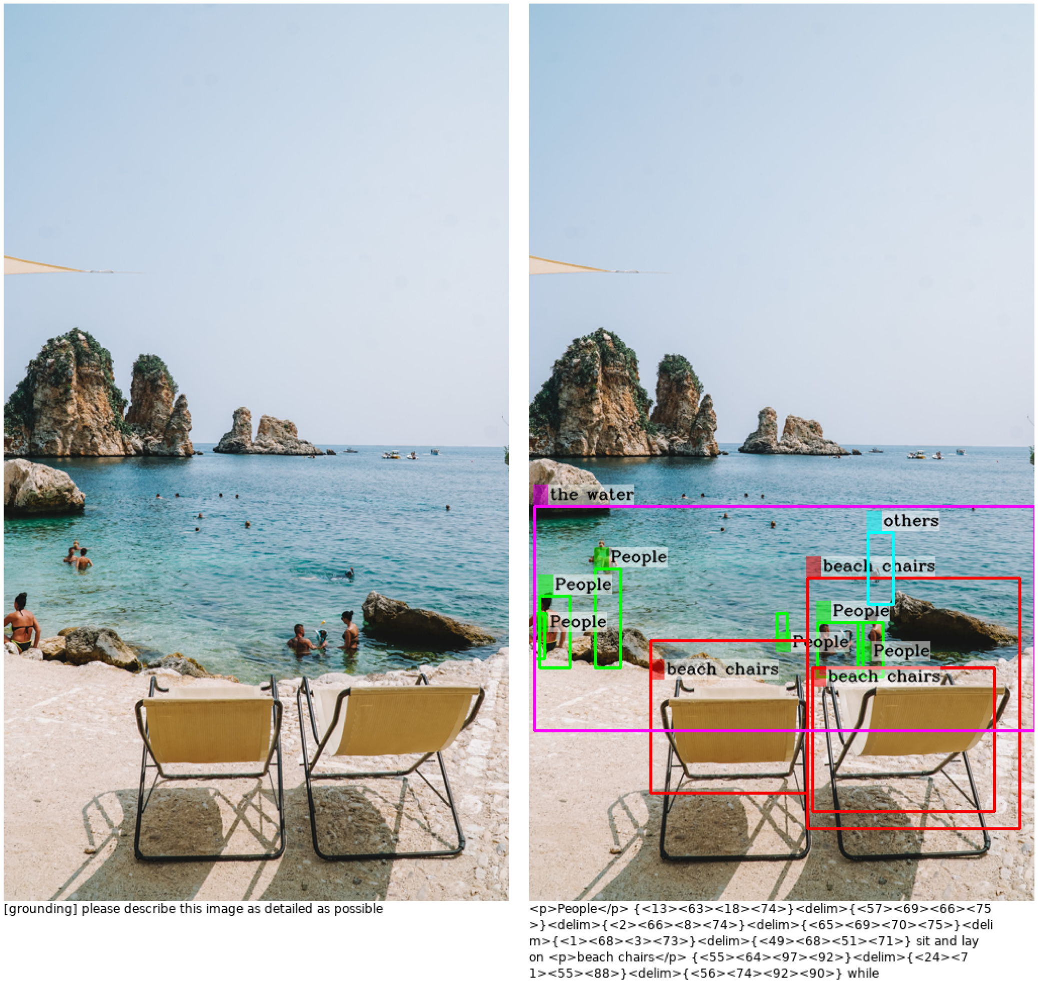

[grounding] please describe this image as detailed as possible

```
<p>People</p> {<13><63><18><74>}<delim>{<57><69><66><75
>}<delim>{<2><66><8><74>}<delim>{<65><69><70><75>}<deli
m>{<1><68><3><73>}<delim>{<49><68><51><71>} sit and lay
on <p>beach chairs</p> {<55><64><97><92>}<delim>{<24><7
1><55><88>}<delim>{<56><74><92><90>} while
```

Figure 7: Detail grounded image caption example

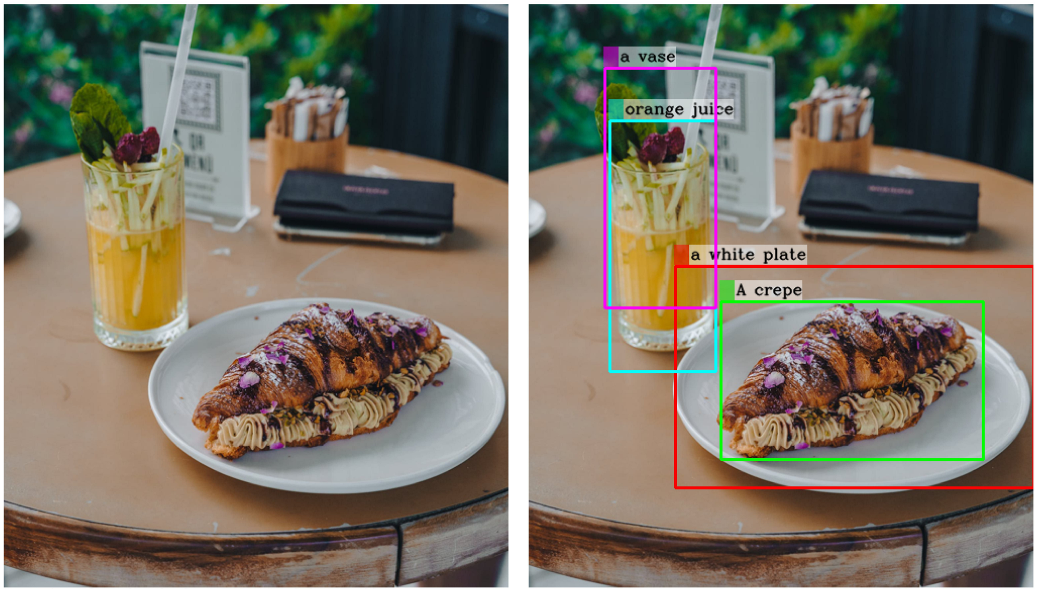

[grounding] please describe this image as detailed as possible

<p>A crepe</p> {<38><51><90><78>} sits on <p>a white plate</p> {<29><45><100><83>} near a cup of <p>orange juice</p> {<16><20><37><63>} and <p>a vase</p> {<15><11><37><52>} with a stem in the background .

Figure 8: Detail grounded image caption example

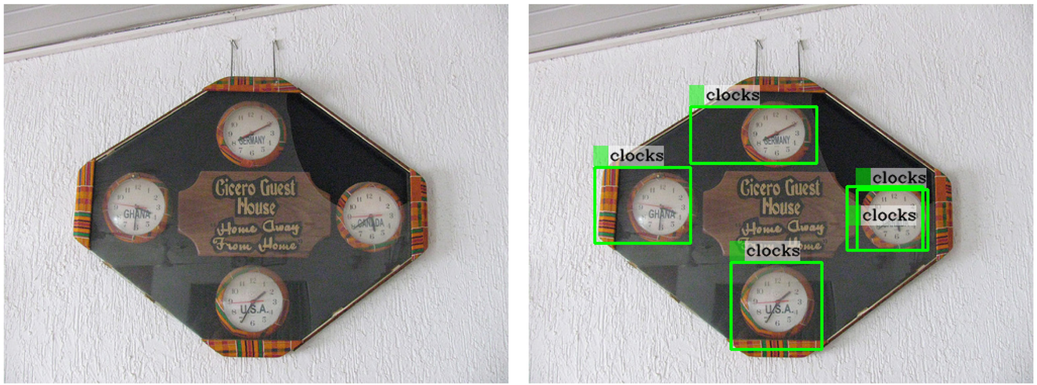

[detection] clocks

<p>clocks</p> {<40><68><58><91>}<delim>{<32><27><57><42>}<delim>{<13><43><32><63>}<delim>{<65><49><79><65>}<delim>{<63><48><78><65>}

Figure 9: Object parsing and grounding example

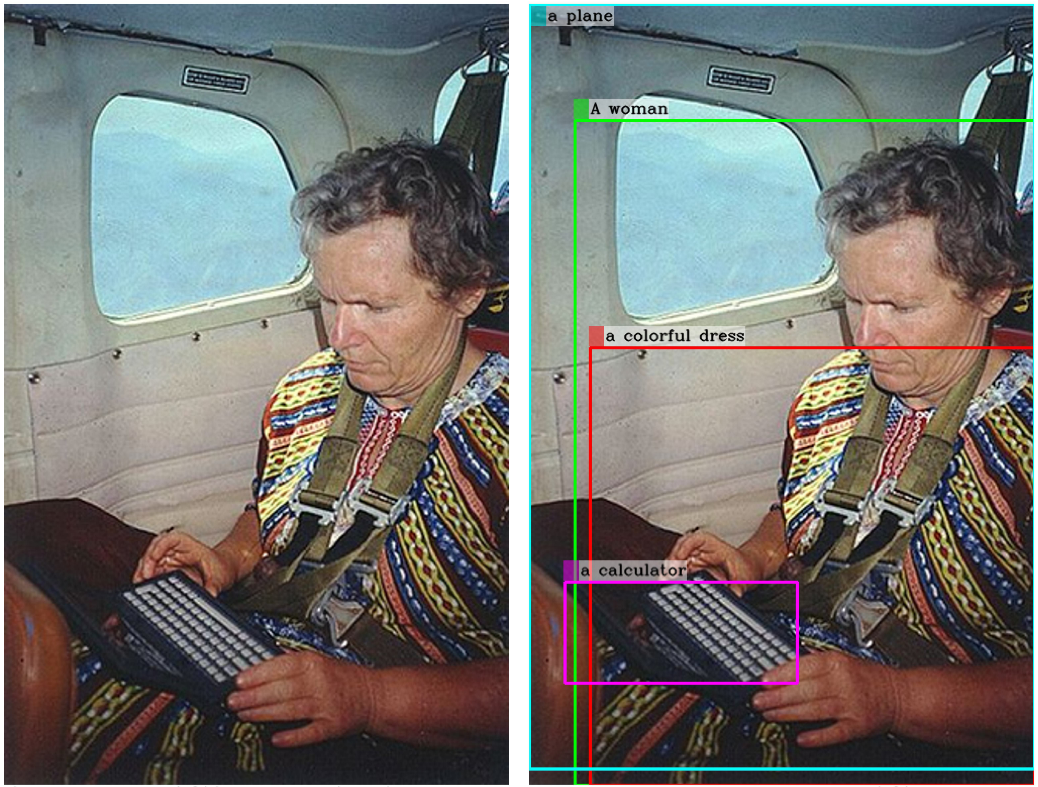

[detection] A woman in a colorful dress is sitting in a plane and typing on a calculator

<p>A woman</p> {<9><15><100><100>} <p>a colorful dress</p> {<12><44><100><100>} <p>a plane</p> {<0><0><100><98>} <p>a calculator</p> {<7><74><53><87>}

Figure 10: Object parsing and grounding example

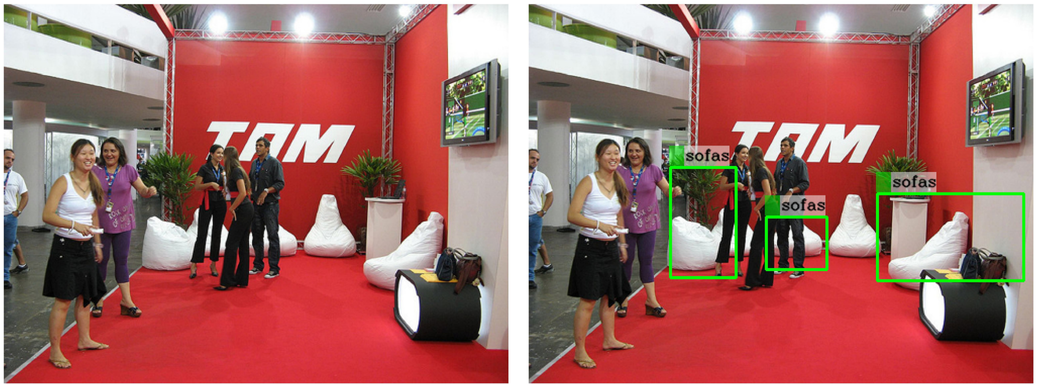

[detection] sofas

<p>sofas</p> {<28><43><41><72>}<delim>{<69><50><98><73>}<delim>{<47><56><59><70>}

Figure 11: Object parsing and grounding example

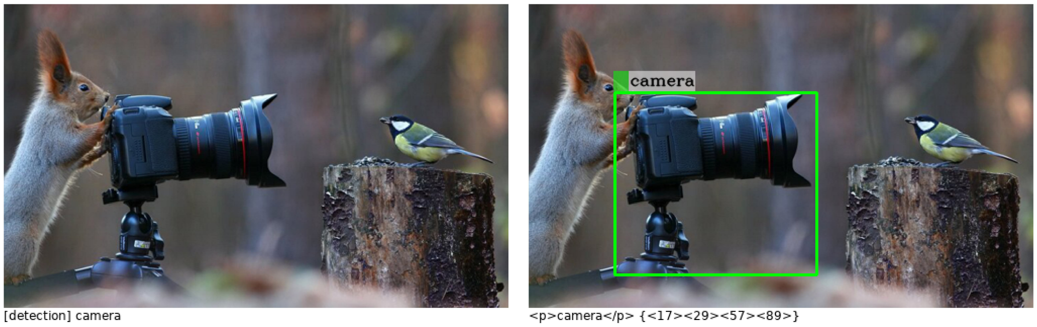

[detection] camera

<p>camera</p> {<17><29><57><89>}

Figure 12: Object parsing and grounding example

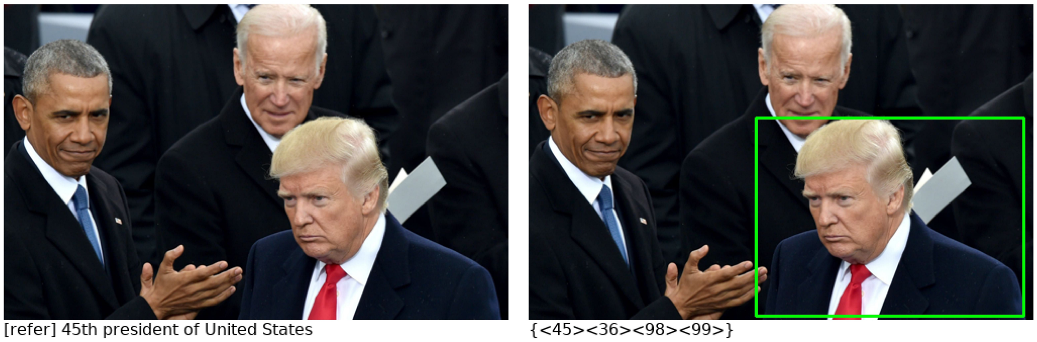

[refer] 45th president of United States

{<45><36><98><99>}

Figure 13: Referring expression comprehension example

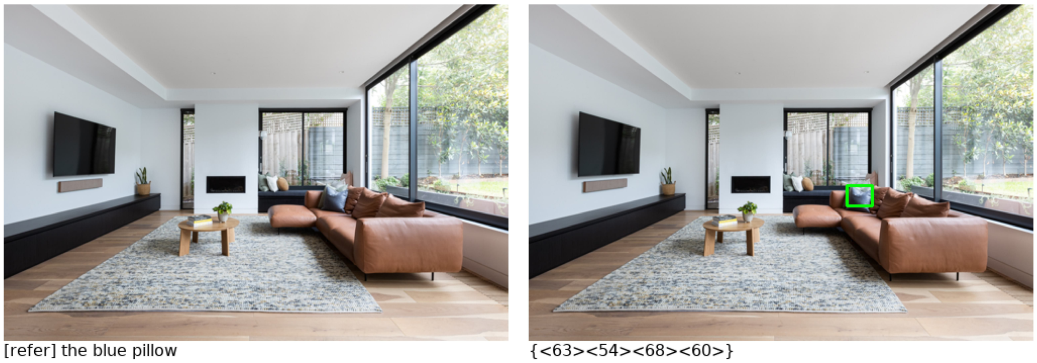

[refer] the blue pillow

{<63><54><68><60>}

Figure 14: Referring expression comprehension example

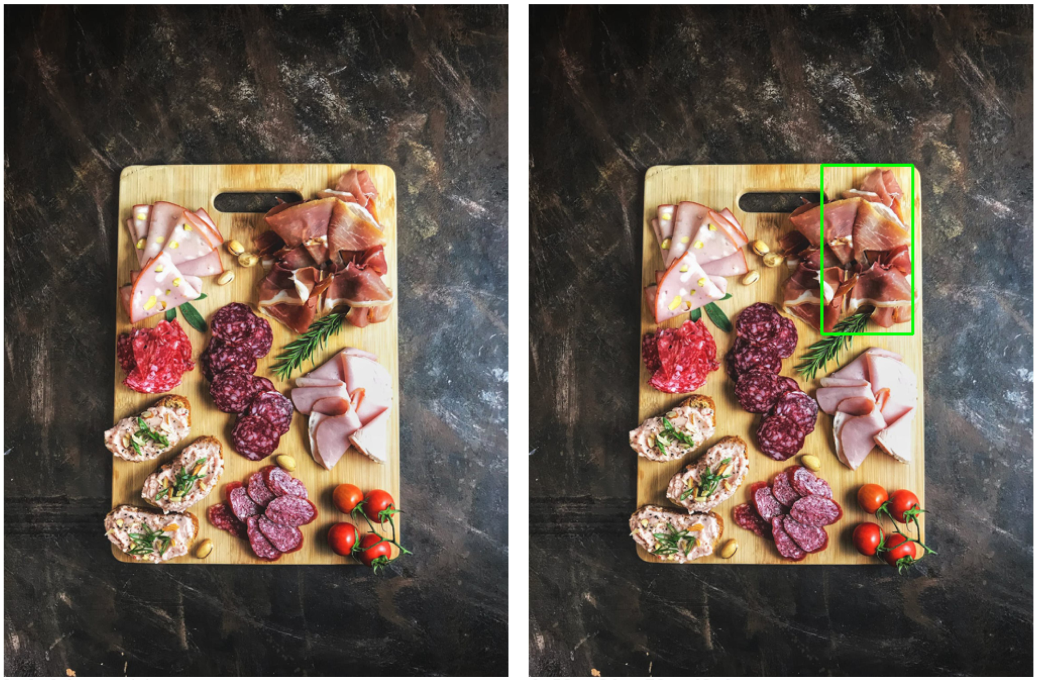

[refer] the top right meat

{<58><24><76><49>}

Figure 15: Referring expression comprehension example

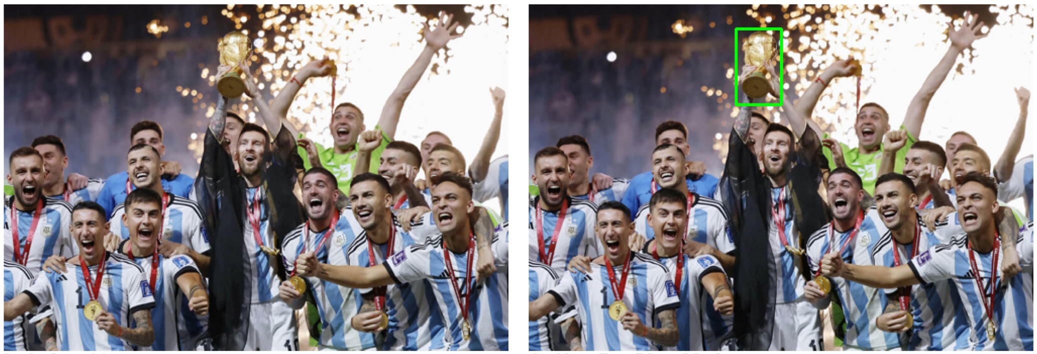

[refer] world cup

{<41><7><50><29>}

Figure 16: Referring expression comprehension example

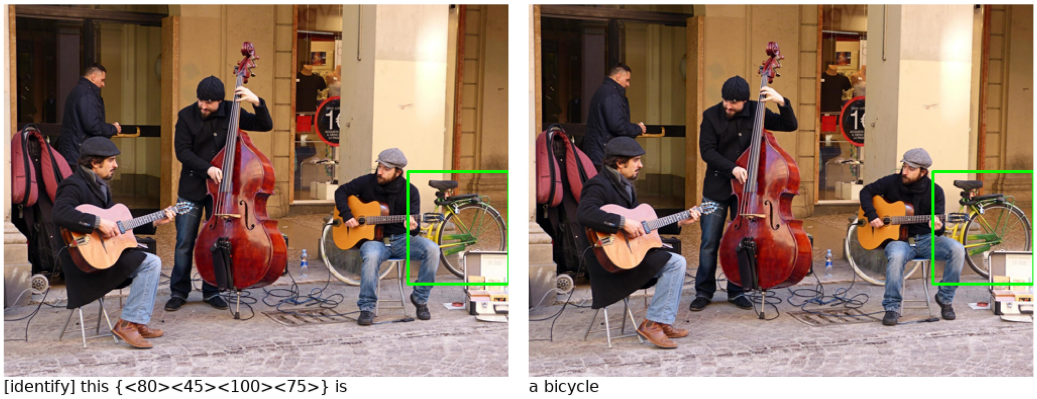

Figure 17: object identification example

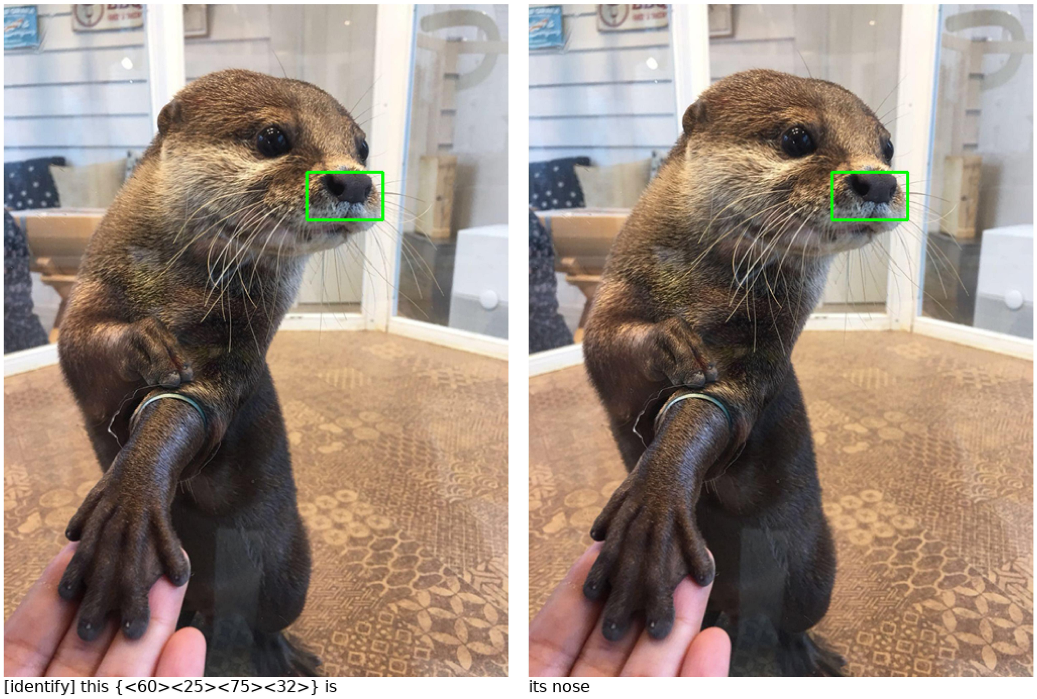

Figure 18: object identification example

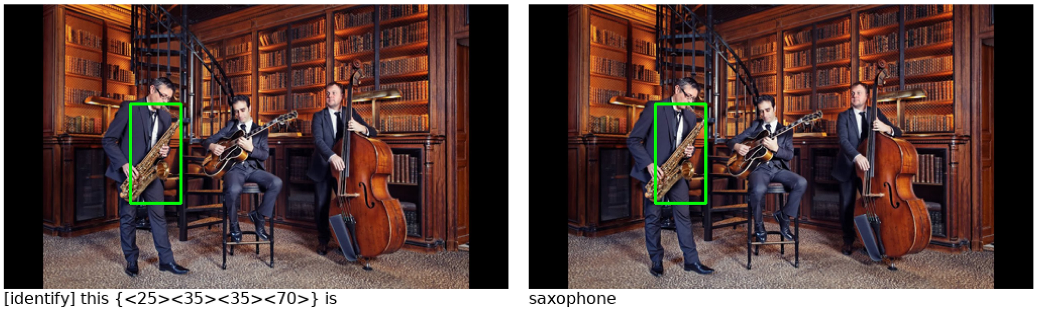

Figure 19: object identification example

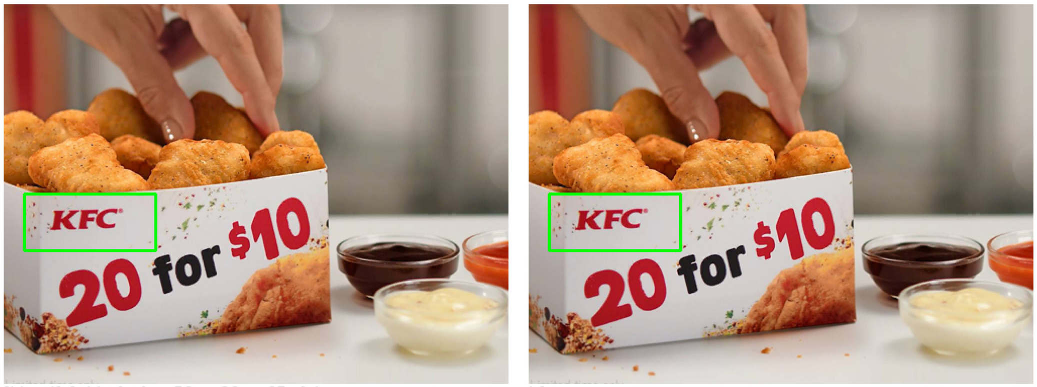

[identify] this {<4><50><30><65>} is

kfc

Figure 20: object identification example

REFERENCES

Jean-Baptiste Alayrac, Jeff Donahue, Pauline Luc, Antoine Miech, Iain Barr, Yana Hasson, Karel Lenc, Arthur Mensch, Katherine Millican, Malcolm Reynolds, et al. Flamingo: a visual language model for few-shot learning. In *Advances in Neural Information Processing Systems*, 2022.

Jinze Bai, Shuai Bai, Shusheng Yang, Shijie Wang, Sinan Tan, Peng Wang, Junyang Lin, Chang Zhou, and Jingren Zhou. Qwen-vl: A frontier large vision-language model with versatile abilities. *arXiv preprint arXiv:2308.12966*, 2023.

Tom Brown, Benjamin Mann, Nick Ryder, Melanie Subbiah, Jared D Kaplan, Prafulla Dhariwal, Arvind Neelakantan, Pranav Shyam, Girish Sastry, Amanda Askell, et al. Language models are few-shot learners. *Advances in neural information processing systems*, 33:1877–1901, 2020.

Jun Chen, Han Guo, Kai Yi, Boyang Li, and Mohamed Elhoseiny. Visualgpt: Data-efficient adaptation of pretrained language models for image captioning. In *Proceedings of the IEEE/CVF Conference on Computer Vision and Pattern Recognition*, pp. 18030–18040, 2022.

Jun Chen, Deyao Zhu, Kilichbek Haydarov, Xiang Li, and Mohamed Elhoseiny. Video chatcaptioner: Towards the enriched spatiotemporal descriptions. *arXiv preprint arXiv:2304.04227*, 2023a.

Keqin Chen, Zhao Zhang, Weili Zeng, Richong Zhang, Feng Zhu, and Rui Zhao. Shikra: Unleashing multimodal llm's referential dialogue magic. *arXiv preprint arXiv:2306.15195*, 2023b.

Wei-Lin Chiang, Zhuohan Li, Zi Lin, Ying Sheng, Zhanghao Wu, Hao Zhang, Lianmin Zheng, Siyuan Zhuang, Yonghao Zhuang, Joseph E. Gonzalez, Ion Stoica, and Eric P. Xing. Vicuna: An open-source chatbot impressing gpt-4 with 90%* chatgpt quality, March 2023. URL `https://vicuna.lmsys.org`.

Aakanksha Chowdhery, Sharan Narang, Jacob Devlin, Maarten Bosma, Gaurav Mishra, Adam Roberts, Paul Barham, Hyung Won Chung, Charles Sutton, Sebastian Gehrmann, et al. Palm: Scaling language modeling with pathways. *arXiv preprint arXiv:2204.02311*, 2022.

Wenliang Dai, Junnan Li, Dongxu Li, Anthony Meng Huat Tiong, Junqi Zhao, Weisheng Wang, Boyang Li, Pascale Fung, and Steven Hoi. Instructblip: Towards general-purpose vision-language models with instruction tuning, 2023.

Jacob Devlin, Ming-Wei Chang, Kenton Lee, and Kristina Toutanova. Bert: Pre-training of deep bidirectional transformers for language understanding. *arXiv preprint arXiv:1810.04805*, 2018.

Yuxin Fang, Wen Wang, Binhui Xie, Quan Sun, Ledell Wu, Xinggang Wang, Tiejun Huang, Xinlong Wang, and Yue Cao. Eva: Exploring the limits of masked visual representation learning at scale. *arXiv preprint arXiv:2211.07636*, 2022.

Zhe Gan, Yen-Chun Chen, Linjie Li, Chen Zhu, Yu Cheng, and Jingjing Liu. Large-scale adversarial training for vision-and-language representation learning. *Advances in Neural Information Processing Systems*, 33: 6616–6628, 2020.

Tao Gong, Chengqi Lyu, Shilong Zhang, Yudong Wang, Miao Zheng, Qian Zhao, Kuikun Liu, Wenwei Zhang, Ping Luo, and Kai Chen. Multimodal-gpt: A vision and language model for dialogue with humans. *arXiv preprint arXiv:2305.04790*, 2023.

Yash Goyal, Tejas Khot, Douglas Summers-Stay, Dhruv Batra, and Devi Parikh. Making the v in vqa matter: Elevating the role of image understanding in visual question answering. In *Proceedings of the IEEE conference on computer vision and pattern recognition*, pp. 6904–6913, 2017.

Danna Gurari, Qing Li, Abigale J Stangl, Anhong Guo, Chi Lin, Kristen Grauman, Jiebo Luo, and Jeffrey P Bigham. Vizwiz grand challenge: Answering visual questions from blind people. In *Proceedings of the IEEE conference on computer vision and pattern recognition*, pp. 3608–3617, 2018.

Or Honovich, Thomas Scialom, Omer Levy, and Timo Schick. Unnatural instructions: Tuning language models with (almost) no human labor. *arXiv preprint arXiv:2212.09689*, 2022.

Edward J Hu, Yelong Shen, Phillip Wallis, Zeyuan Allen-Zhu, Yuanzhi Li, Shean Wang, Lu Wang, and Weizhu Chen. Lora: Low-rank adaptation of large language models. *arXiv preprint arXiv:2106.09685*, 2021.

Ronghang Hu and Amanpreet Singh. Unit: Multimodal multitask learning with a unified transformer. In *Proceedings of the IEEE/CVF International Conference on Computer Vision*, pp. 1439–1449, 2021.

Drew A Hudson and Christopher D Manning. Gqa: A new dataset for real-world visual reasoning and compositional question answering. In *Proceedings of the IEEE/CVF conference on computer vision and pattern recognition*, pp. 6700–6709, 2019.

Gabriel Ilharco, Mitchell Wortsman, Ross Wightman, Cade Gordon, Nicholas Carlini, Rohan Taori, Achal Dave, Vaishaal Shankar, Hongseok Namkoong, John Miller, Hannaneh Hajishirzi, Ali Farhadi, and Ludwig Schmidt. Openclip, July 2021. URL `https://doi.org/10.5281/zenodo.5143773`. If you use this software, please cite it as below.

Sahar Kazemzadeh, Vicente Ordonez, Mark Matten, and Tamara Berg. Referitgame: Referring to objects in photographs of natural scenes. In *Proceedings of the 2014 conference on empirical methods in natural language processing (EMNLP)*, pp. 787–798, 2014.

Douwe Kiela, Hamed Firooz, Aravind Mohan, Vedanuj Goswami, Amanpreet Singh, Pratik Ringshia, and Davide Testuggine. The hateful memes challenge: Detecting hate speech in multimodal memes. *Advances in neural information processing systems*, 33:2611–2624, 2020.

Bo Li, Yuanhan Zhang, Liangyu Chen, Jinghao Wang, Jingkang Yang, and Ziwei Liu. Otter: A multi-modal model with in-context instruction tuning. *arXiv preprint arXiv:2305.03726*, 2023a.

Dongxu Li, Junnan Li, Hongdong Li, Juan Carlos Niebles, and Steven CH Hoi. Align and prompt: Video-and-language pre-training with entity prompts. In *Proceedings of the IEEE/CVF Conference on Computer Vision and Pattern Recognition*, pp. 4953–4963, 2022.

Junnan Li, Dongxu Li, Silvio Savarese, and Steven Hoi. Blip-2: Bootstrapping language-image pre-training with frozen image encoders and large language models. *arXiv preprint arXiv:2301.12597*, 2023b.

Xiujun Li, Xi Yin, Chunyuan Li, Pengchuan Zhang, Xiaowei Hu, Lei Zhang, Lijuan Wang, Houdong Hu, Li Dong, Furu Wei, et al. Oscar: Object-semantics aligned pre-training for vision-language tasks. In *Computer Vision–ECCV 2020: 16th European Conference, Glasgow, UK, August 23–28, 2020, Proceedings, Part XXX 16*, pp. 121–137. Springer, 2020.

Yifan Li, Yifan Du, Kun Zhou, Jinpeng Wang, Wayne Xin Zhao, and Ji-Rong Wen. Evaluating object hallucination in large vision-language models. *arXiv preprint arXiv:2305.10355*, 2023c.

Tsung-Yi Lin, Michael Maire, Serge Belongie, James Hays, Pietro Perona, Deva Ramanan, Piotr Dollár, and C Lawrence Zitnick. Microsoft coco: Common objects in context. In *Computer Vision–ECCV 2014: 13th European Conference, Zurich, Switzerland, September 6-12, 2014, Proceedings, Part V 13*, pp. 740–755. Springer, 2014.

Fangyu Liu, Guy Emerson, and Nigel Collier. Visual spatial reasoning. *Transactions of the Association for Computational Linguistics*, 11:635–651, 2023a.

Haotian Liu, Chunyuan Li, Qingyang Wu, and Yong Jae Lee. Visual instruction tuning. *arXiv preprint arXiv:2304.08485*, 2023b.

Shilong Liu, Zhaoyang Zeng, Tianhe Ren, Feng Li, Hao Zhang, Jie Yang, Chunyuan Li, Jianwei Yang, Hang Su, Jun Zhu, et al. Grounding dino: Marrying dino with grounded pre-training for open-set object detection. *arXiv preprint arXiv:2303.05499*, 2023c.

Jiasen Lu, Christopher Clark, Rowan Zellers, Roozbeh Mottaghi, and Aniruddha Kembhavi. UNIFIED-IO: A unified model for vision, language, and multi-modal tasks. In *The Eleventh International Conference on Learning Representations*, 2023. URL `https://openreview.net/forum?id=E01k9048soZ`.

Pan Lu, Liang Qiu, Jiaqi Chen, Tony Xia, Yizhou Zhao, Wei Zhang, Zhou Yu, Xiaodan Liang, and Song-Chun Zhu. Iconqa: A new benchmark for abstract diagram understanding and visual language reasoning. *arXiv preprint arXiv:2110.13214*, 2021.

Junhua Mao, Jonathan Huang, Alexander Toshev, Oana Camburu, Alan L Yuille, and Kevin Murphy. Generation and comprehension of unambiguous object descriptions. In *Proceedings of the IEEE conference on computer vision and pattern recognition*, pp. 11–20, 2016.

Kenneth Marino, Mohammad Rastegari, Ali Farhadi, and Roozbeh Mottaghi. Ok-vqa: A visual question answering benchmark requiring external knowledge. In *Proceedings of the IEEE/cvf conference on computer vision and pattern recognition*, pp. 3195–3204, 2019.

Anand Mishra, Shashank Shekhar, Ajeet Kumar Singh, and Anirban Chakraborty. Ocr-vqa: Visual question answering by reading text in images. In *2019 international conference on document analysis and recognition (ICDAR)*, pp. 947–952. IEEE, 2019.

OpenAI. Introducing chatgpt. *https://openai.com/blog/chatgpt*, 2022.

OpenAI. Gpt-4 technical report, 2023.

Vicente Ordonez, Girish Kulkarni, and Tamara Berg. Im2text: Describing images using 1 million captioned photographs. *Advances in neural information processing systems*, 24, 2011.

Zhiliang Peng, Wenhui Wang, Li Dong, Yaru Hao, Shaohan Huang, Shuming Ma, and Furu Wei. Kosmos-2: Grounding multimodal large language models to the world. *arXiv preprint arXiv:2306.14824*, 2023.

Bryan A Plummer, Liwei Wang, Chris M Cervantes, Juan C Caicedo, Julia Hockenmaier, and Svetlana Lazebnik. Flickr30k entities: Collecting region-to-phrase correspondences for richer image-to-sentence models. In *Proceedings of the IEEE international conference on computer vision*, pp. 2641–2649, 2015.

Alec Radford, Jeffrey Wu, Rewon Child, David Luan, Dario Amodei, Ilya Sutskever, et al. Language models are unsupervised multitask learners. *OpenAI blog*, 1(8):9, 2019.

Alec Radford, Jong Wook Kim, Chris Hallacy, Aditya Ramesh, Gabriel Goh, Sandhini Agarwal, Girish Sastry, Amanda Askell, Pamela Mishkin, Jack Clark, et al. Learning transferable visual models from natural language supervision. In *International conference on machine learning*, pp. 8748–8763. PMLR, 2021.

Anna Rohrbach, Lisa Anne Hendricks, Kaylee Burns, Trevor Darrell, and Kate Saenko. Object hallucination in image captioning. *arXiv preprint arXiv:1809.02156*, 2018.

Christoph Schuhmann, Richard Vencu, Romain Beaumont, Robert Kaczmarczyk, Clayton Mullis, Aarush Katta, Theo Coombes, Jenia Jitsev, and Aran Komatsuzaki. Laion-400m: Open dataset of clip-filtered 400 million image-text pairs. *arXiv preprint arXiv:2111.02114*, 2021.

Dustin Schwenk, Apoorv Khandelwal, Christopher Clark, Kenneth Marino, and Roozbeh Mottaghi. A-okvqa: A benchmark for visual question answering using world knowledge. In *European Conference on Computer Vision*, pp. 146–162. Springer, 2022.

Piyush Sharma, Nan Ding, Sebastian Goodman, and Radu Soricut. Conceptual captions: A cleaned, hypernymed, image alt-text dataset for automatic image captioning. In *Proceedings of the 56th Annual Meeting of the Association for Computational Linguistics (Volume 1: Long Papers)*, pp. 2556–2565, 2018.

Oleksii Sidorov, Ronghang Hu, Marcus Rohrbach, and Amanpreet Singh. Textcaps: a dataset for image captioningwith reading comprehension. 2020.

Amanpreet Singh, Vivek Natarajan, Meet Shah, Yu Jiang, Xinlei Chen, Dhruv Batra, Devi Parikh, and Marcus Rohrbach. Towards vqa models that can read. In *Proceedings of the IEEE/CVF conference on computer vision and pattern recognition*, pp. 8317–8326, 2019.

Amanpreet Singh, Ronghang Hu, Vedanuj Goswami, Guillaume Couairon, Wojciech Galuba, Marcus Rohrbach, and Douwe Kiela. Flava: A foundational language and vision alignment model. In *Proceedings of the IEEE/CVF Conference on Computer Vision and Pattern Recognition*, pp. 15638–15650, 2022.

Hugo Touvron, Thibaut Lavril, Gautier Izacard, Xavier Martinet, Marie-Anne Lachaux, Timothée Lacroix, Baptiste Rozière, Naman Goyal, Eric Hambro, Faisal Azhar, et al. Llama: Open and efficient foundation language models. *arXiv preprint arXiv:2302.13971*, 2023a.

Hugo Touvron, Louis Martin, Kevin Stone, Peter Albert, Amjad Almahairi, Yasmine Babaei, Nikolay Bashlykov, Soumya Batra, Prajjwal Bhargava, Shruti Bhosale, et al. Llama 2: Open foundation and fine-tuned chat models. *arXiv preprint arXiv:2307.09288*, 2023b.

Maria Tsimpoukelli, Jacob L Menick, Serkan Cabi, SM Eslami, Oriol Vinyals, and Felix Hill. Multimodal few-shot learning with frozen language models. *Advances in Neural Information Processing Systems*, 34: 200–212, 2021.

Peng Wang, An Yang, Rui Men, Junyang Lin, Shuai Bai, Zhikang Li, Jianxin Ma, Chang Zhou, Jingren Zhou, and Hongxia Yang. Ofa: Unifying architectures, tasks, and modalities through a simple sequence-to-sequence learning framework. In *International Conference on Machine Learning*, pp. 23318–23340. PMLR, 2022a.

Peng Wang, Shijie Wang, Junyang Lin, Shuai Bai, Xiaohuan Zhou, Jingren Zhou, Xinggang Wang, and Chang Zhou. One-peace: Exploring one general representation model toward unlimited modalities. *arXiv preprint arXiv:2305.11172*, 2023a.

Wenhai Wang, Zhe Chen, Xiaokang Chen, Jiannan Wu, Xizhou Zhu, Gang Zeng, Ping Luo, Tong Lu, Jie Zhou, Yu Qiao, et al. Visionllm: Large language model is also an open-ended decoder for vision-centric tasks. *arXiv preprint arXiv:2305.11175*, 2023b.

Wenhui Wang, Hangbo Bao, Li Dong, Johan Bjorck, Zhiliang Peng, Qiang Liu, Kriti Aggarwal, Owais Khan Mohammed, Saksham Singhal, Subhojit Som, et al. Image as a foreign language: Beit pretraining for all vision and vision-language tasks. *arXiv preprint arXiv:2208.10442*, 2022b.

Hu Xu, Saining Xie, Xiaoqing Ellen Tan, Po-Yao Huang, Russell Howes, Vasu Sharma, Shang-Wen Li, Gargi Ghosh, Luke Zettlemoyer, and Christoph Feichtenhofer. Demystifying clip data. *arXiv preprint arXiv:2309.16671*, 2023a.

Peng Xu, Wenqi Shao, Kaipeng Zhang, Peng Gao, Shuo Liu, Meng Lei, Fanqing Meng, Siyuan Huang, Yu Qiao, and Ping Luo. Lvlm-ehub: A comprehensive evaluation benchmark for large vision-language models. *arXiv preprint arXiv:2306.09265*, 2023b.

Bin Yan, Yi Jiang, Jiannan Wu, Dong Wang, Ping Luo, Zehuan Yuan, and Huchuan Lu. Universal instance perception as object discovery and retrieval. In *Proceedings of the IEEE/CVF Conference on Computer Vision and Pattern Recognition*, pp. 15325–15336, 2023.

Qinghao Ye, Haiyang Xu, Guohai Xu, Jiabo Ye, Ming Yan, Yiyang Zhou, Junyang Wang, Anwen Hu, Pengcheng Shi, Yaya Shi, et al. mplug-owl: Modularization empowers large language models with multimodality. *arXiv preprint arXiv:2304.14178*, 2023.

Jiahui Yu, Zirui Wang, Vijay Vasudevan, Legg Yeung, Mojtaba Seyedhosseini, and Yonghui Wu. Coca: Contrastive captioners are image-text foundation models. *arXiv preprint arXiv:2205.01917*, 2022.

Licheng Yu, Patrick Poirson, Shan Yang, Alexander C Berg, and Tamara L Berg. Modeling context in referring expressions. In *Computer Vision–ECCV 2016: 14th European Conference, Amsterdam, The Netherlands, October 11-14, 2016, Proceedings, Part II 14*, pp. 69–85. Springer, 2016.

Lu Yuan, Dongdong Chen, Yi-Ling Chen, Noel Codella, Xiyang Dai, Jianfeng Gao, Houdong Hu, Xuedong Huang, Boxin Li, Chunyuan Li, et al. Florence: A new foundation model for computer vision. *arXiv preprint arXiv:2111.11432*, 2021.

Pengchuan Zhang, Xiujun Li, Xiaowei Hu, Jianwei Yang, Lei Zhang, Lijuan Wang, Yejin Choi, and Jianfeng Gao. Vinvl: Revisiting visual representations in vision-language models. In *Proceedings of the IEEE/CVF conference on computer vision and pattern recognition*, pp. 5579–5588, 2021.

Deyao Zhu, Jun Chen, Kilichbek Haydarov, Xiaoqian Shen, Wenxuan Zhang, and Mohamed Elhoseiny. Chatgpt asks, blip-2 answers: Automatic questioning towards enriched visual descriptions. *arXiv preprint arXiv:2303.06594*, 2023a.

Deyao Zhu, Jun Chen, Xiaoqian Shen, Xiang Li, and Mohamed Elhoseiny. Minigpt-4: Enhancing vision-language understanding with advanced large language models. *arXiv preprint arXiv:2304.10592*, 2023b.

Mingchen Zhuge, Haozhe Liu, Francesco Faccio, Dylan R Ashley, Róbert Csordás, Anand Gopalakrishnan, Abdullah Hamdi, Hasan Abed Al Kader Hammoud, Vincent Herrmann, Kazuki Irie, et al. Mindstorms in natural language-based societies of mind. *arXiv preprint arXiv:2305.17066*, 2023.